BRNO UNIVERSITY OF TECHNOLOGY

FACULTY OF ELECTRICAL ENGINEERING
AND COMMUNICATION

DEPARTMENT OF TELECOMMUNICATIONS

Ing. Kryštof Zeman

MODELING OF MMWAVE PROPAGATION CHANNEL FOR OFF-BODY COMMUNICATION SCENARIOS

MODELOVÁNÍ PROPAGAČNÍHO KANÁLU PRO OFF-BODY KOMUNIKACI V OBLASTI MILIMETROVÝCH VLN

SHORTENED VERSION OF PH.D. THESIS

Specialization:	Teleinformatics
Supervisor:	doc. Ing. Jiří Hošek, Ph.D.
Opponents:	Prof. Ing. Miroslav Vozňák , Ph.D.
	Prof. Yuliya Gaidamaka, Ph.D.
Date of Defense:	14. 9. 2019

KEYWORDS

Channel modeling, mmWave, NS-3, Simulation, 5G, BAN, Body shadowing, Signal propagation, Off-body communication

KLÍČOVÁ SLOVA

Modelování přenosových kanálů, mmWave, NS-3, Simulace, BAN, Útlum lidského těla, Propagace signálu, Off-body komunikace

ARCHIVED IN

Dissertation is available at the Science Department of Dean's Office FEEC, Brno University of Technology, Technická 10, Brno, 616 00

MÍSTO ULOŽENÍ PRÁCE

Disertační práce je k dispozici na Vědeckém oddělení děkanátu FEKT VUT v Brně, Technická 10, Brno, 616 00

ISBN 80-214-
ISSN 1213-4198

OBSAH

1 MOTIVATION

The first part of this section will be dedicated to the motivation of this thesis, where the current status of the Body Area Networks (BANs) is described. The focus will be given onto the novel areas that are arising and their specifics. Furthermore, second part of this section will continue with detailed description of current imperfections and challenges that will be further studied in this thesis. The area of interest, which was further divided into sub-goals is also described here.

1.1 Motivation

The communication technologies have been rapidly evolving during the past decade raising the demand for reliable and high speed communication. This demand is driven by the never-ending search of better quality of life and the advancements in almost all technology fields. Even more, with the recent boom in the online High Definition (HD) content streaming and applications of Augmented Reality (AR) and Virtual Reality (VR), the demand for very high throughput over short distances had risen exponentially (for AR and VR technologies specifically, Cisco forecasts 12-fold increase in global throughput from 2017 to 2022 [1]). To cope with these changes, the communication technologies in Local Area Networks (LANs) and BANs are still undergoing transformation from wired to wireless solutions. This BANs idea currently comprehends a wide variety of devices ranging from the sensors deployed on a human body or in the clothes fabric, that are measuring vital signals of a human body and thus providing valuable information for medical diagnosis, sports statistics and other leisure as well as professional activity reports, to a more bulky wearable devices, such as AR and VR glasses that are providing entertainment, information and industrial applications. All these devices have one key requirement in common – the radio link between them and the remote concentrator / access point needs to be very robust to fulfill the Quality of Experience (QoE) and to allow seamless transition to the already ongoing "smart" revolution, which is currently represented by the idea of smart cities and smart households. The unique placement of the devices (see Fig. 1.1) implies the need for a study of the signal propagation aspects, more precisely a proper channel characterization. This dissertation thesis is motivated by this vision of futuristic wireless system, which will be most probably part of the upcoming 5G systems, where the devices will be deployed on a human body and their wireless connectivity will enhance the user capabilities and quality of life by allowing users to be online anytime, anywhere and instantly [2].

The BANs are described as an extension of Wide Area Networks (WANs) to a personal sphere. They can be further divided into four distinct types:

- **In-Body** communications that occur between two or more devices inside a human body. This communication is mostly between implanted medical sensors and majority of the transmission path is inside the human body.
- **On-Body** communications are happening within the networks and wearable systems in direct proximity of human body. That means both Transceiver (Tx) and Receiver (Rx) are located directly on or very near the human body. Most of the communication channel is characterized by the propagation on the surface of human body.
- **Body-to-Body** communications appear between antennas placed on two or more separated human bodies. The communication principle is similar to the off-body case, but in body-to-body communication the antennas are influenced by the user body on both ends.
- **Off-Body** communications are made between the devices placed on a human body and devices placed on a remote Access Point (AP). Most of the channel is therefore represented by free space propagation and off body link.

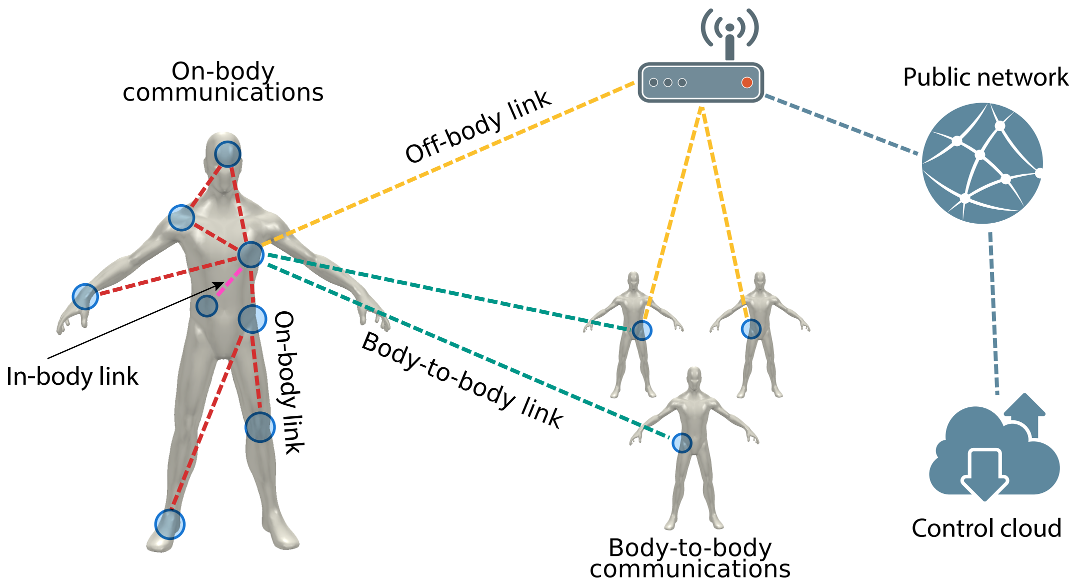

Fig. 1.1: Body-centric communication.

This thesis is focused on the off-body communication from the BAN domain. On-body and in-body communications are not covered as it would involve a comprehensive investigation of the insight of human body, which is clearly out of scope of this work.

As aforementioned, body centric communications are nowadays covering all fields of the market. The most known usages are in health-care, where BAN can be used to monitor health and motion information in real-time, sending the readings to the nearby diagnostic or storage devices, from which they can be further processed. This can not only significantly improve quality of life of patients that need constant monitoring of vital signals such as Electrocardiogram (ECG), Electroencephalography (EEG), respiratory rate, heart rate, etc., but also save time of medical personnel. Furthermore, with the rapid improvements in the hardware design, the devices are getting much smaller and some of the functions are being implemented in consumer-grade technologies (e.g., Apple Watch[1]).

In military and emergency services, the wearable sensors can be used to track users motion, Global Positioning System (GPS) position, and vital signals. This can be further utilized to specialized suits that can monitor bullet wounds and share the position of the user with other soldiers [3] or, in case of firefighters, measure heat and toxicity levels together with providing important information about people and objects that cannot be seen due to the low visibility levels[2]. For such cases, the communication link reliability is critical as any connection failure can be fatal.

For the secure authentication, BANs promise a new possibilities in form of biometric sensing. They can be used for both physiological and behavioral schemes creation, such as facial patterns, iris and fingerprints recognition. These techniques are recently being prone to forgery and duplicability, which motivated the investigations of new physical and behavioral characteristics of the human body, such as EEG and multimodal biometric systems. These authentication methods can also be used for daily life applications such as shopping (credit card authentication).

In sports, the BANs may be used for motion and vital signal monitoring. These measurements of fitness-related activities often include evaluation of heart rate, limbs position, energy consumption or fat percentage. Based on results from the measurements, data are displayed real-time to the user or are further evaluated by specialized software / personnel to optimize the athletes performance.

In both the entertainment and industrial applications, the trend is now clear – the multimedia future is wireless and belongs mostly to the AR and VR technologies. This means the communication requirements are vastly different from the aforementioned usages. The communication usually requires real-time high speed transfer of voice, video and data together, but on the contrary it is not so prone to packet loss and the security is also not so critical. Best example of this use case is the VR headset that is streaming high quality audio and video from the central unit to its inbuilt display and speakers.

In all aforementioned applications, the radio channel plays a key role in the over-

[1] https://www.apple.com/apple-watch-series-4/health/ with integrated ECG
[2] https://www.qwake.tech/

all system performance. The radio channel and signal propagation was extensively investigated over more than 2 decades. The technologies and standards underwent a big change during that time, evolving from the 2G, 3G and 4G to current 5G mobile communications. Together with the new standards, the supporting technologies also evolved, resulting in a myriad of channel models ranging from simple to sophisticated ones. Some of these models were results of European co-operation projects such as European Cooperation in Science and Technology (COST) 207, 231, 259, 273, 2100, IC 1004, or the European Telecommunications Standards Institute (ETSI), the Third Generation Partnership Project (3GPP) and Institute of Electrical and Electronics Engineers (IEEE) group 802 and therefore incorporated as part of them. Based on these projects, it can be concluded that there is quite profound knowledge of the outdoor channels (urban, suburban and rural) concerning the communication between mobile terminals and base stations. On the other side, most of these projects were done for the lower frequency bands of the Industrial, Scientific and Medical (ISM) spectrum. This means that there is still a lot of potential in the BANs and the higher frequency bands in the ISM spectra.

The goal of this thesis is to focus on BAN radio channeling issues, with accent given to the off-body communication at millimeter wave frequencies. The target is to create a channel model representing the communication link between the antenna on a user body and the antenna on the remote base station. The model will be further implemented into well-known NS3 to extend current model created by the New York University (NYU) and will enable more efficient and precise simulation of the indoor propagation.

1.2 Novelty and Research Goals

As it was mentioned in the Section. 1, the current evolution of high-speed wireless networks raised the demand for the higher throughput, lower latency networks. This sudden change increased the network scarcity that spread over multiple subgroups of devices which share the same transmission media – the wireless spectrum. The most interesting and up-to-date area of interest is the one comprised of BAN devices for VR and AR technologies and devices and applications alike [4]. Unfortunately, as aforementioned, these devices are demanding higher throughput and lower latency that the traditional ISM wireless networks can offer. To overcome these limits of the lower ISM frequency bands, there is undergoing shift to millimeter wave spectrum, which is still underutilized and able to offer two aforementioned key parameters: much wider bandwidths and lower latency [5]. Due to the complexity of this task, it has to be splitted into minor goals that will help to overcome a selected issue, together forming a complete solution. One of this sub-tasks is to create a channel model that will help the scientific community to speed up the prototyping phase of new devices and planning of the devices / Base Station (BS) deployment. The main goals of this dissertation are therefore focused on the channel modeling issue, which is further divided into following sub-goals:

- Extensive study of currently available and researched high-speed wireless standards and technologies focused on the BAN.
- Evaluation of currently utilized mmWave network standards with a close attention given to the channel models.
- Based on the previous step, creation of mmWave BAN specific custom channel model to improve the simulation accuracy.
- Evaluation of the model against field measurements. Calibration of the parameters.
- Implementation of the created channel model into the NS3 simulator.
- Utilization of the NS3 simulator for a variety of simulation scenarios to provide an overview of the selected parameters impact on the signal propagation (i.e., different room sizes)

All of these tasks will be covered by this thesis, providing an comprehensive insight into the stated problem. Furthermore, the possible solutions for increasing the model accuracy and effectivity will be given together with an recommendations, how to extend it in the future.

2 DESIGNED CHANNEL MODEL FOR MMWAVES

This chapter will focus on designed in-detail mmWave channel modeling scenario. The reason for this scenario is mainly the fact, that there are very few works targeting the body shadowing modeling in off-body mmWave spectrum scenarios. Furthermore, most of these models are utilizing static transmitter and receiver or focus on communication between vehicles. Even fewer scientific works consider scenarios with mobile devices (such as hand-held phones) operated by dynamic users. They are further restricted to forward motion with constant velocity and do not account for body postures [6].

2.1 Reference Scenario

The reference scenario is focusing on indoor off-body communication, represented by a rectangular room with predefined measures The idea of this scenario is to model the propagation loss of mobile terminals and devices that are operating in near proximity of a human body (such as hand-held phones) or directly on it (AR/VR glasses, sensors, etc.) that are communicating with the static wall-mounted BS.

2.1.1 Scenario Layout

As aforementioned, the footprint of the scenario was chosen to be rectangular, representing the most common room shapes. The measures of the room were further adjusted to simulate specific cases such as closet (4 x 2 m), study room (10 x 6 m), and seminar room closet (12 x 20 m). As the inside objects of the room, such as wallpapers, posters, image frames, and other types of traditional room equipment are specific to each room, it was decided to simulate them using probability function. Other items inside the rooms are omitted for the time being, but are planned to be added in future work.

The position of the User Equipment (UE) antenna is dynamic and can be placed at any location inside the room, therefore effectively simulating user movement. The BS position is fixed, representing a wall-mounted BS, as it would be in a real scenario. Similarly, the height of the UE antenna is 1.6 m from ground, which is the statistical average of human height. The height of the BS antenna is set to 2 m, which is the usual height of the antenna placed on the wall or near the ceiling. The UE antennas are further divided into several on-body locations (see Fig. 2.1):

- Head, where the antenna can be put either on left (He_L) or right side (He_R)

- Chest, where the antenna is placed directly on user's middle chest from the front (To_F) or back side (To_B)
- Wrist, where the antenna is situated at the right arm of the user (Wr_R)

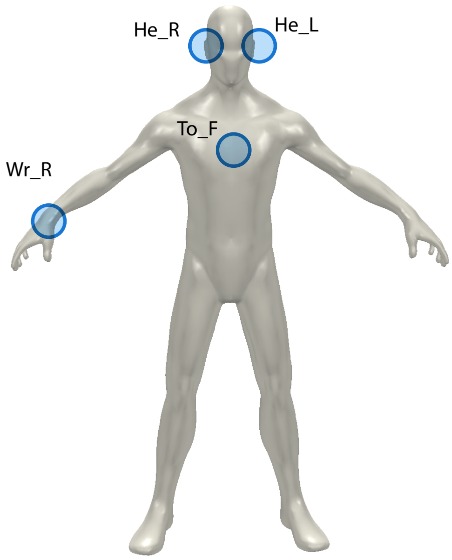

Fig. 2.1: Antenna placement on the user's body.

Based on the human dynamics, the UE antennas are always modeled as dynamically moving (due to the subtle body movements such as breathing). This means the antenna elevation and azimuth angles are again modeled by a random distribution.

2.1.2 Channel Model Implementation

The created channel model itself is divided into several parts that represent each of the phenomenons that influence the signal loss. The founding idea of this thesis is to create modularized model that incorporates the most influential large and small scale fading parameters. In this section we provide detailed description of each part to illustrate the complexity of the model and to provide better understanding of each part of the implementation.

The first part is dedicated to creation of the core of the model. Its main purpose is the path loss calculation. It accounts for four rays at total. First ray is the direct ray representing the line of sight connection between the transmitter and receiver. This can be defined by modified Free Space Path Loss (FSPL) formula:

$$H(t) = \frac{\lambda}{4\pi d}\sqrt{G_t G_r}\mathrm{e}^{-j\frac{2\pi d}{\lambda}}, \tag{2.1}$$

where H represents the amplitude (transmittance), the λ is wavelength, d distance between the transmitter and receiver, G_t and G_r are transmitting and receiving gain, respectively, and the $e^{-j\frac{2\pi d}{\lambda}}$ accounts for the signal phase. The same principle is used for the other three rays, each of them representing reflection from one wall. In addition to the path loss generated by the aforementioned FSPL formula, the reflected rays are also attenuated by the reflection loss. This loss was added as:

$$|\Gamma| = U(0.6, 0.8), \tag{2.2}$$

where the $|\Gamma|$ represents the reflection loss and the U represents uniform distribution. This loss is material-dependent, usually in range from 0.6 to 0.8 for the mmWave frequencies [7]. More information about the material dependency and reflection principles can be found in full version of the thesis. Furthermore, the reflection on the incident object causes phase shift that can be generally added as random variable to the phase of the ray. This influence comes from the wavelength of the mmWave signals and the great variance of the phase coupled with it. Therefore the reflection randomness was added as:

$$Refl_{rand} = U(0, 2\pi). \tag{2.3}$$

The last part is dedicated to the body shadowing on the user side. This is one of the most neglected loss and also one of the most important losses when it comes to simulation of user mobility. Presented model utilizes the shadowing function created in [8]. This shadowing function was originally developed for lower frequencies, but we further adjusted it for millimeter waves. The body shadowing loss is modeled as:

$$S(d,\phi)_{[\mathrm{dB}]} = S_m(d)_{[\mathrm{dB}]}\frac{1}{2}\left(1 + \cos\frac{2\pi}{\Delta\phi}\left(\phi - \phi_0\right)\right), \tag{2.4}$$

where S_m is maximum body-shadowing loss, $\Delta\phi$ is the shadowing pattern width, ϕ is the azimuth angle of departure, ϕ_0 is azimuth angle of maximum loss represented as:

$$\phi_0 = \phi_a + \pi, \tag{2.5}$$

where ϕ_u is the maximum radiation antenna orientation angle in Global Coordinate System (GCS) and the π represents the exact opposite orientation, therefore providing the maximum loss angle. Together all aforementioned parts can be expressed as:

$$P_{r_{[\mathrm{dBm}]}} = P_{t_{[\mathrm{dBm}]}} - L_{sf_{[\mathrm{dB}]}}, \tag{2.6}$$

where the P_r and P_t are transmitting and received power respectively and the L_{path} is the shadowing loss expressed as:

$$L_{sf_{[\mathrm{dB}]}} = -20 \log_{10} \left| \sum_{i=0}^{n} H_i 10^{\frac{S(d,\phi)_{[\mathrm{dB}]}}{-20}} |\Gamma| \right|, \tag{2.7}$$

where $S(d,\phi)_{[\mathrm{dB}]}$ equals to:

$$S(d,\phi)_{[\mathrm{dB}]} = S_m(d)_{[\mathrm{dB}]} \frac{1}{2} \left(1 + \cos \frac{2\pi}{\Delta\phi} (\phi - \phi_0) \right), \tag{2.8}$$

where S_m is maximum body-shadowing loss, $\Delta\phi$ is the shadowing pattern width, ϕ is the azimuth angle of departure, ϕ_0 is azimuth angle of maximum loss. This resulting formula can be used to simulate the complex propagation inside rooms of variable sizes.

2.1.3 Channel Model Optimization

The developed model, which was introduced in Section 2.1.2 was further utilized to simulate user movement inside three different rooms of predefined sizes (2x4 m, 6x10 m, 12x20 m). The goal was to approximate the propagation attenuation by less complex function and to approximate the fading by a distribution function. The methodology of fitting is described in further paragraphs.

For each of the aforementioned room sizes, three different base station positions were chosen: (i) in the middle of right room, (ii) top right corner, and (iii) middle of the top wall. The user's position was chosen to be on lanes positioned at $y/16$ increments to cover gradually increasing reflection angles and the accompanied prolonged propagation distances (see Fig. 2.2).

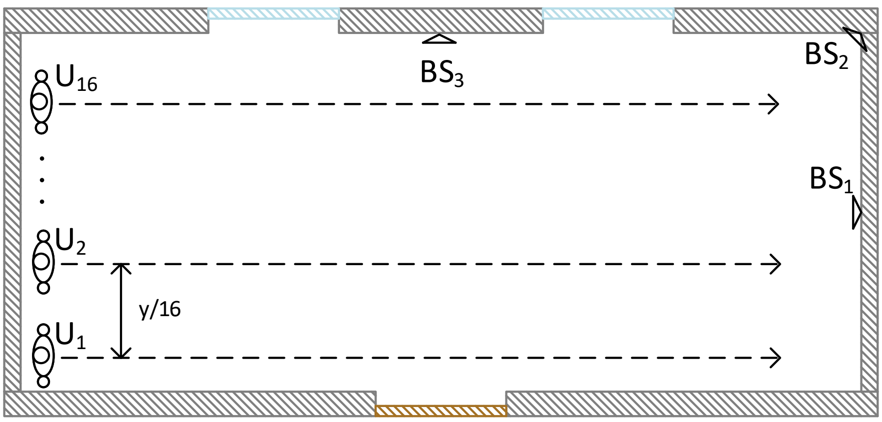

Fig. 2.2: Base station and user equipment positions utilized for the model optimization.

For each set of aforementioned data, the linear scale pathloss component was calculated using the 2.1, 2.2 and 2.3 formulas. Then for each lane, the pathloss was approximated by a curve using following formula:

$$y = \frac{\alpha}{x^{\beta}}, \tag{2.9}$$

where α and β are slope and shape coefficients, respectively and x is the distance in meters. Using the resulting curve, the shadowing variation was found. The shadowing was further fitted to a number of different distributions (Rician, Rayleigh, Stable, Normal, Logistic) in order to find the best correlation for each line segment in the room. To compare goodness of the fit of all aforementioned distributions, standard evaluation metrics were used in following order: (i) Standard correlation statistics with threshold of 0.95 for first, quick sorting, and then (ii) Chi-squared statistics with 0.05 significance of goodness of the fit to further evaluate the goodness of the fitting process. After calculating the distribution coefficients per each line (y/16 m step) segment, the resulting data were averaged and used to generate the resulting coefficients used in the model for the shadowing.

Based on the overall averaged results provided in a sample Tab.2.1 (complete list of tables is provided the attachments), we can conclude that if we compare the goodness of the fit for selected distributions purely by the correlation coefficient, the Normal distribution provides best fit for the most cases with the average correlation coefficient of 0.796, closely followed by the Rice distribution. If we compare the goodness of the fit using more complex methods, such as Chi^2 statistics, the Normal distribution is still the most satisfying, again very closely followed by Rice distribution.

Tab. 2.1: Distribution fitting of proposed model results

Distribution	**Chi^2 order**	**Corr order**	**Chi^2 stat**	**Chi^2 crit**	**Chi^2 p value**	**Correlation**
Normal	3.00	3.00	802.65	64.00	0.00	0.90
Rayleigh	7.00	7.00	9191.35	65.17	0.00	0.40
Logistic	5.00	5.00	1198.04	64.00	0.00	0.88
Stable	2.00	2.00	800.21	61.66	0.00	0.90
Rice	1.00	1.00	800.07	64.00	0.00	0.90
Nakagami	4.00	4.00	1039.85	64.00	0.00	0.89
Lognormal	6.00	6.00	2373.50	64.00	1.41	0.83

Based on the aforementioned table, we consider a Rice distribution as the best one for further simulations. Furthermore, to be able to recreate the original signal, the curve got from 2.9 were converted into dB and fitted to common log-distance pathloss formula:

$$L_p = L_{p_{d_0}} + 10n \log_{10} \frac{d_i}{d_0} + L_{sf}, \tag{2.10}$$

where $L_{p_{d0}}$ is pathloss at reference distance d_0 (1 m), n is the pathloss exponent, d_i is the distance in meters, and L_{sf} is the shadowing coefficient which was added after the fitting as:

$$L_{sf} = R(s, \sigma), \tag{2.11}$$

where $R(s, \sigma)$ is the Rician distribution with s standing for noncentrality parameter, modelled as a mean of all partial noncentrality parameters s_part that resulted from the different y positions and the σ representing the shadowing variation. The resulting parameters used for further simulations are grouped for each room size, antenna position of the UE and BS and frequency, presented in the attached files.

Tab. 2.2: Pathloss and Rician coefficients for room size of 4x2 m with reflection coefficient of 0.4-0.6

	BS position [m]									
Tx position	**[4,1]**					**[4,2]**				
	$L_{p_{d_0}}$ [dB]	n	s	sigma	corr	$L_{p_{d_0}}$ [dB]	n	s	sigma	corr
TO_F	67.84	1.92	0.96	0.29	0.94	67.84	1.89	0.94	0.33	0.93
HE_L	67.87	2.00	0.99	0.17	0.84	67.64	2.06	0.98	0.18	0.91
HE_R	67.96	2.00	0.99	0.12	0.90	67.87	2.01	0.99	0.13	0.89
WR_R	67.94	1.98	0.99	1.15	0.93	67.86	2.00	0.98	0.17	0.94
TO_B						68.04	1.96	0.99	0.18	0.97

Based on the results (sample data can be seen in Tab. 2.2) it can be seen that the rooms size does not play major role in the pathloss estimation. Oppositely, the BS location affects the pathloss more significantly. This can be seen for the cases, where the BS is shifted from the center right position of the room to upper right corner (the second column in all aforementioned Tables). Also, the antenna position can play an important role, when placed on specific locations such as TO_F and HE_L/HE_R. Interestingly, when utilizing the antenna position on the wrist (WR_R), the signal attenuation has generally having smaller pathloss exponent than the head antenna position. This is due to the fact, that the hand is periodically moving and therefore the body attenuation is not taking place all the time. Furthermore, to provide more graphical illustration of the channel model functionality, complex pathloss map for a room of size 10x6 m is provided in Fig. 2.3.

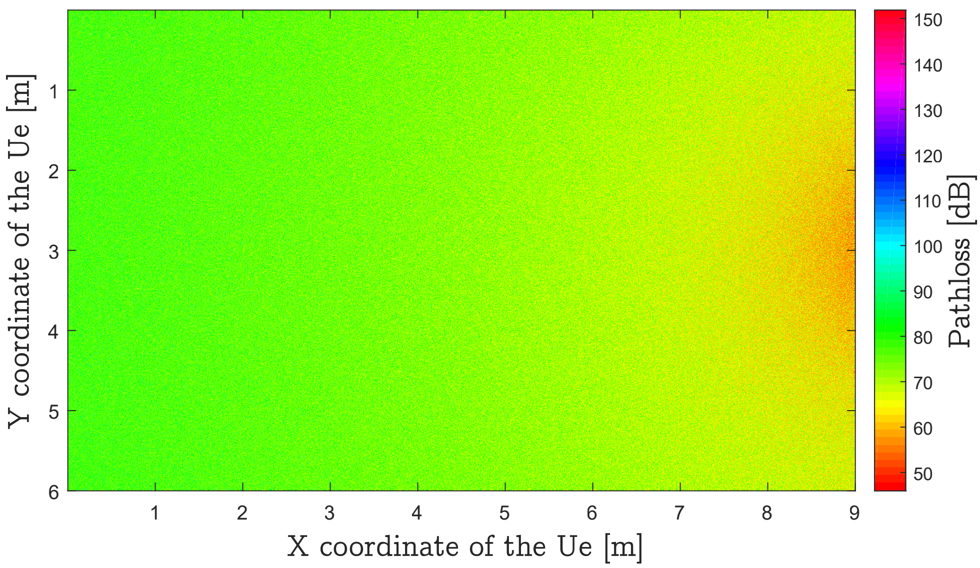

Fig. 2.3: Pathloss distribution inside a room of size 10x6 m.

As it can be seen in Fig. 2.3, the BS is static at [10,3] coordinates, while the theoretical UE can be at any point ranging from [0,0] to [9,6] coordinates. This effectively produces a map of all points inside the room (except the ones that are from 9 meters further apart), showing the complex propagation characteristics. The model presented in this section and its utilization for simulations is further published in [9].

3 ANALYSIS OF CHANNEL MODEL BEHAVIOR USING THE CUSTOM MODEL

The model created in Section 2 and further evaluated, as described in full version of this thesis, is utilized to analyze the channel behavior in this section. The idea of further described scenarios is to provide a detailed analysis of the signal propagation in indoor environment that consists of static obstacles (walls) and dynamic user with mobile antenna. The model is further implemented into the NS3 simulator, but thanks to its mathematical nature, it can be easily implemented into any other simulation tool. In the first section of this chapter, brief introduction into the structure of utilized NS3 module is given. In latter sections, the simulated scenarios and results are discussed.

3.1 Advancements of the NS3 mmWave Module

Due to the aforementioned restrictions of the NS3 mmWave module, it was decided to update its structure. Firstly, the attention was given to the accuracy comparison of the NS3 mmWave channel models. In [10], it was identified that all the implemented channel models did not take into account the thickness of blockage objects. This lead to the overly optimistic propagation in case of strong block objects such as steel door. To mitigate this issue, a simple limit-power policy was proposed to simulate the outage events more accurately.

This idea was further extended in [11], where the limit power policy was substituted by more sophisticated algorithm, which is accounting for the blockage object thickness. This extension enables users to simulate scenarios with multiple blockage objects of different thicknesses shadowing the Line of Sight (LOS) of the transmitter. The simulation results prove the importance of the accounting for the thickness of the object.

Finally, this model was further adjusted in [12] to account also for the material of the blocker. This enabled users to distinguish between not only thickness of the blocker, but also between the materials, from which was the blocker made. This is especially beneficial for diversification of the materials inside the room, where there are often metal or concrete walls, but the inside of the rooms is furnished with wooden closets. To further illustrate the importance of this approach, the results are depicted in Fig. 3.1.

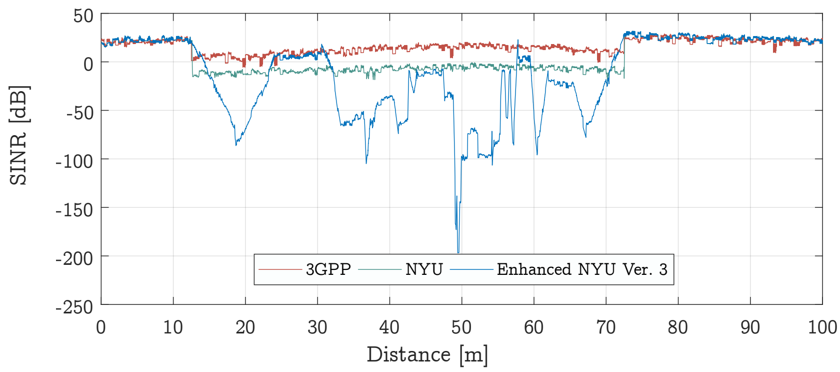

Fig. 3.1: Simulation results of complex building with different materials used for walls.

3.2 Extension of the NS3 Propagation Model

To successfully implement our model into the NS3 simulator, the mmWave module had to be adjusted accordingly. Thanks to the modularity of the NS3 and its derived modules, the changes were made in the `BuildingsObstaclePropagationLossModel` class. This class, similarly to the whole mmWave module, was created by the authors from [13]. Its main purpose is to provide detailed propagation loss model for scenarios that take buildings into the account. It is further divided into three sub-scenarios based on the position of nodes: (i) outdoor scenario, where both UE and BS are outside the buildings, (ii) indoor to outdoor scenario, where either the UE or BS is inside and the other one is in the opposite environment, and (iii) indoor scenario, where both UE and BS are inside a building. As our model is primarily focused on the indoor off-body propagation channel, we added the option (iii) and modified its content to utilize our proposed model from Section 2.1.2.

3.3 Simulated Scenarios

As discussed in the Section 1, the need for accurate and reliable simulation of the mmWave networks is still unsatisfied. This section is proposing a model scenarios that are covering all tunable parameters of created channel model, providing a in-depth insights into how each parameter influences the simulation. If all these scenarios are combined, they simulate real-life scenarios as closely as possible.

3.3.1 Simulation Parameters

To effectively verify the validity of each of the setup parameters for selected simulation scenarios, it was needed to unify all remaining parameters that are not used to describe the scenarios' parameters. Therefore for all the simulations inside this section, the simulation settings were set as described in Tab. 3.1.

Tab. 3.1: Simulation scenarios' parameters

Parameter name	**Set value**
Center frequency	60 GHz
Tx power	1 dBm
Rx power	1 dBm
Tx gain	1 dBm
Rx gain	1 dBm
TCP segment size	1400 b
HARQ	Enabled
Chunk per RB	144
Bandwidth	2 GHz

This data was selected to simulate the current IEEE 802.11ad standard as closely as possible. The utilized bandwidth was setup to the similar size of 2 GHz and the rest of the settings are set to default.

3.3.2 Different Room Dimensions

The biggest disadvantage of mmWave spectrum is its high atmospheric loss, which effectively attenuates the signals over bigger distances. This effect is especially strong around the 60 GHz frequency, which, in combination with the reflection loss can be critical inside a larger rooms such as airport lounges or seminar rooms. This subsection is dedicated to modeling the effect of different room sizes on the propagation attenuation and transmission speed.

Utilizing the created channel model, we have tasted three different room sizes to evaluate the impact on the network performance. The room sizes, which are illustrated in Fig. 3.2, were: (4x2 m, 10x6 m and 20x12 m). The user was moving towards the BS positioned at the middle of the furthest wall (see Fig. 3.2 for reference). By taking this approach, it was possible to simulate the pathloss decay for all three rooms, effectively preserving the baseline for the comparison. The channel coefficients, corresponding to each room size were taken from Section 2.1.3.

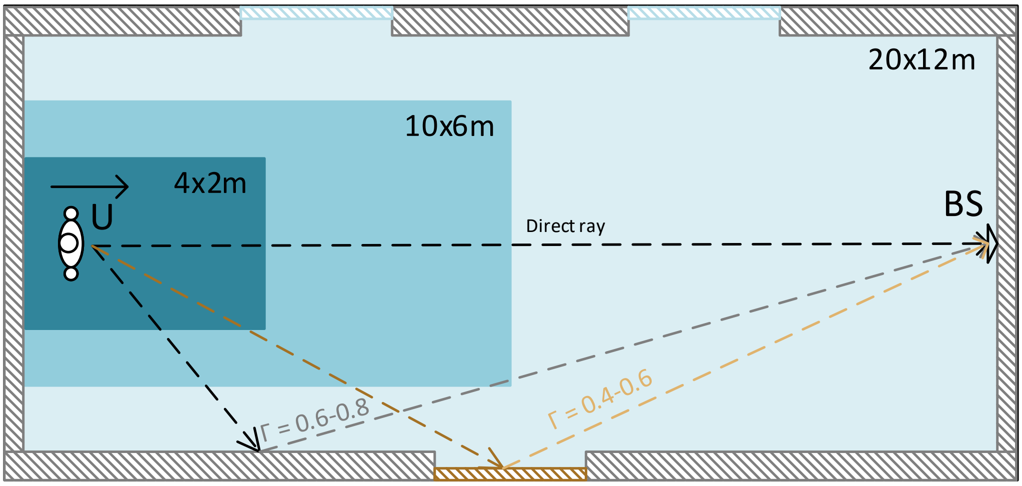

Fig. 3.2: SINR value estimates based on our proposed channel model.

The simulation results are depicted in Fig. 3.3. It can clearly be seen that the room sizes up to 20 m do play a minor role in the signal attenuation, resulting usually in about less than half of dB difference. On the contrary, the antenna location and

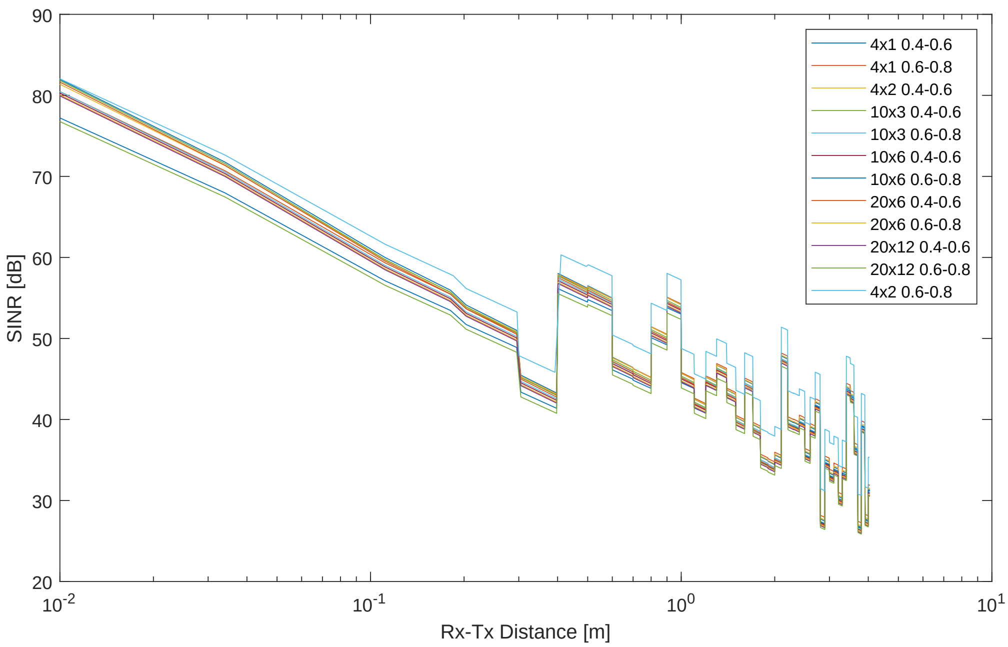

Fig. 3.3: SINR value estimates based on our proposed channel model.

the reflection coefficient can play a significant role, providing bigger loss when the location is incorrect. For example, the Signal to Interference plus Noise Ratio (SINR) difference between the two antenna placements inside a room of 20x12 m is almost a 1 dB. If a stronger reflection loss is added to this scenario, the SINR will be better by more than 2 dB. Even though all aforementioned differences may seem negligible in comparison to the variance shown in Fig. 3.3, it has to be noted that with much larger rooms and communication on greater distances, the attenuation will increase drastically. This trend is visible from the Fig. 3.3 as well, showing the difference between the smallest room with smaller reflection coefficients and the largest room with the stronger reflection coefficients to be almost 10 dB.

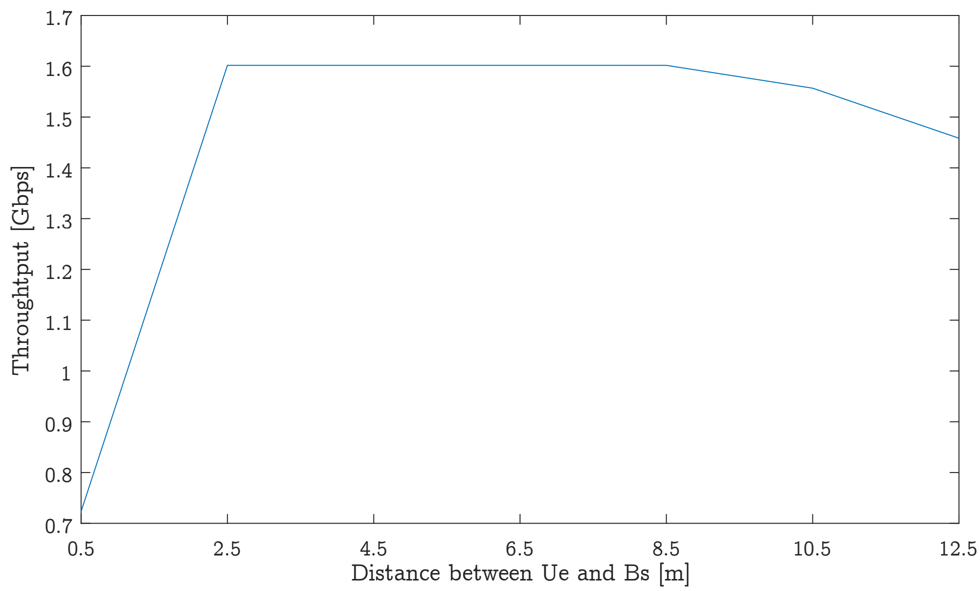

Fig. 3.4: Round Trip Time (RTT) of scenario with one UE and one BS.

Furthermore, if we take the same models and add an attenuation of 20 dB, which was measured as a average attenuation done by blocking human body, and increase the transmission distance, the results are much more interesting. This behavior can be seen in Fig. 3.4, where the ramp up in the beginning is again caused by the Transmission Control Protocol (TCP) initialization process, where it adjusts the transmission parameters to fully utilize the available bandwidth. Also, it can be seen that the throughput begins to decrease after 9 m, based on which it can be concluded that for larger rooms with a random human blockage (i.e., airport halls, larger offices, etc.), it will be vital to utilize higher gain antennas together with complex beamforming algorithms.

Based on all the aforementioned simulation results, it can be stated that for the fast prediction of channel behavior inside a rooms up to size of 20x12 m, all the developed channel parameters can be used. Furthermore, if they will be approximated into the single value, it can be used for a even faster, rough estimation of the channel quality. For more detailed and accurate simulation, the correct parameters from Section 2.1.3 have to be taken. Also, it should be noted that the model is not in the final state and further development is planned to provide more flexible simulation and more accurate results.

4 CONCLUSION

The rapid evolution of BANs caused by the new revolutionary applications such as AR and VR is driving the next stage of wireless networks. These networks are expected to be interconnected with the cellular systems, together creating a next-generation (5G) wireless systems. Their main advantage lies in the manifold increase in data rates, latency and overall QoE. This, as aforementioned, will be extremely beneficial for the novelty applications in health care, industry and entertainment fields. However, to be able to unleash the full potential of these systems, a new frequencies, mainly from the millimeter-wave spectrum need to be utilized. This poses a challenges in the propagation modeling, which was dealt with in this thesis.

Within the full text, the signal propagation at mmWaves is comprehensively described in Chapter 2. The first part of this chapter is dedicated to large scale propagation channel effects, which are vital part of the whole propagation channel. More precisely, the insight into four main channel effects is given. Starting with the log-distance propagation models that are widely used for pathloss decay characterization, the insight into the pathloss exponent estimation and utilization is given. Furthermore, the atmospheric and weather effects are discussed to highlight the importance of the attenuation caused by the water molecules in the air, which is very pronounced especially around the 60 GHz frequencies. This topic is followed by the signal phenomena caused by objects in the signal path. This phenomena becomes much more stronger at higher frequencies, completely changing the material parameters (at lower frequencies, the surface roughness did not play such a significant role in terms of reflection and scattering). In the second part of this chapter, the small scale propagation channel effects are discussed. Beginning with the delay spread, which, as aforementioned, is much higher due to the higher reflection coefficients and much stronger multipath propagation. Lastly, the attention is given to the Doppler effect, which is expected to be 15-30 times greater than at microwave frequencies.

A comprehensive overview of the most advanced mmWave propagation Models is presented in the full text in Chapter 3. These models are further divided into three groups, creating a complete description of currently available propagation models for any type of scenario. Firstly, the attention is given to the most well-known and used models – the outdoor propagation channel models. Here, the detailed description of the 3GPP style models, from which the 3GPP statistical channel model is the most complex. It is defined for frequencies from 6 to 100 GHz with bandwidths up to 10 % of the carrier frequency. The second mentioned model is the New York University model, which is heavily based on the extensive measurements done by the NYU team. This model is composed of two propagation models (LOS and Non Line Of Sight (NLOS)) to provide more accurate results. Further, the vehicle-to-vehicle channel models are discussed to provide an understanding of the vehicular network specifics. The second part of this chapter is dedicated to indoor propagation models, with attention given to the ray-tracing and Rayleigh, Rician and multiwave fading models that are considered a baseline in indoor channel propagation. These models are followed by the IEEE 802.15.3c and IEEE 802.11ad models, which are currently the most advanced models used for mmWave channel modeling. The last section of this chapter is dedicated to the state-of-the-art simulation tools used for mmWave simulation. This section starts with the WSnet simulator, which is very flexible simulation tool, that can be interfaced with many other modules and simulators to provide a complex wireless network nodes simulation. It is followed by the comprehensive overview of Riverbed Modeler and OMNeT++ simulators, which are widely used throughout the scientific and industrial communities. Lastly, the attention is given to NS3 simulator, which is open-source, community backed simulator containing a lot of modules used for wide variety of simulations. This simulator was chosen to be utilized in this thesis for the simulations that are utilizing custom developed channel model.

To be able to provide a valuable channel model for the off-body communication, a profound knowledge of the BANs was necessary. Therefore the Chapter 4 from the full text ,is dedicated to this topic, providing a thorough description of the peculiarities of BAN channel modeling. Firstly, a deep investigation of three different BAN channels is provided. This complete overview of the on-body, off-body and body-to-body channel modeling provides a strong knowledge base for further simulations. Similarly, the human blockage modeling, which is described in detail in following section, provides an insight into the main areas of the body blockage channel models. The last section of this chapter is dedicated to the BAN antennas, which are an essential part of the whole BAN channel modeling.

Utilizing the knowledge from Chapters 2, 3, and 4, from the full version, a custom channel model was designed in Chapter 2 in this shortened thesis. This model is based on the first order reflections ray tracing principle enhanced by the body shadowing function to more accurately simulate the off-body communication scenarios. The model itself was implemented in MATLAB to provide fast and accurate computations. Furthermore, the model was optimized and fitted to a log-distance pathloss formula to allow easy implementation into the simulation tools such as NS3. After the optimization process, the model was verified against three field measurement campaigns that were conducted by the best scientists in the field and their teams (e.g., prof. S. L. Cotton). This verification proved the accuracy of the proposed model, together with the need of having the pathloss parameters created for different simulation scenarios.

The successfully developed and verified model from the Chapter 2 was further implemented into the NS3 simulator in Chapter 3. Before the analysis of the developed model is presented, the detailed description of the NS3 mmWave module is given, focusing on the core parts module, together with Physical Layer (PHY), Media Access Control (MAC), and Radio Link Control (RLC) layers. Furthermore, a short overview of the advancements of the NS3 mmWave module enhancements proposed by the author of this thesis is given. Following these enhancements, the extension which is utilizing the developed indoor off-body channel model is laid out. The last section of the Chapter 3 is providing a in-depth description of plethora of simulations, which were carefully selected in order to provide a complete understanding of how the channel model parameters affect the channel. Based on these results, we can conclude that all the goals of this thesis were successfully accomplished.

As it was aforementioned in previous paragraph, the main goals of the thesis, were successfully completed. The key contributions are summarized as follows:

- The extensive overview and study of currently available and state-of-the-art high speed wireless BAN standards and technologies was performed.
- An in-depth analysis of currently utilized mmWave network standards were studied, witch close attention given to the channel modeling sections.
- Creation of custom channel model, aimed at the simulation accuracy was performed. The developed channel model is offering not only higher accuracy, but also easy implementability into currently available network simulators.
- The developed model was further evaluated against currently available field measurements. Furthermore, its parameters were adjusted to provide even more accurate simulation.
- To improve the usability and user-friendliness, the model was implemented into the NS3 simulator.
- Utilizing the newly available model in the NS3, which was added in previous step, and extensive simulation of selected scenarios was performed. The results provided great insight into the influence of the rooms sizes, reflection coefficients and antenna position on the propagation loss and overall system performance.

BIBLIOGRAPHY

[1] "Cisco Visual Networking Index: Forecast and Trends, 2017–2022 White Paper," 2018.

[2] P. Masek, E. Mokrov, K. Zeman, A. Ponomarenko-Timofeev, A. Pyattaev, S. Nesterov, S. Andreev, J. Hosek, K. Samouylov, and Y. Koucheryavy, "A practical perspective on 5g-ready highly dynamic spectrum management with lsa," *Wireless Communications and Mobile Computing*, vol. 2018, 2018.

[3] J. Rantakokko, J. Rydell, P. Strömbäck, P. Händel, J. Callmer, D. Törnqvist, F. Gustafsson, M. Jobs, and M. Grudén, "Accurate and reliable soldier and first responder indoor positioning: multisensor systems and cooperative localization," *IEEE Wireless Communications*, vol. 18, no. 2, pp. 10–18, 2011.

[4] K. Zeman, P. Masek, J. Hosek, P. Dvorak, R. Josth, and T. Jankech, "Experimental evaluation of technology enablers for cutting edge wearables' applications," in *2016 8th International Congress on Ultra Modern Telecommunications and Control Systems and Workshops (ICUMT)*, pp. 89–93, IEEE, 2016.

[5] K. Zeman, M. Stusek, J. Pokorny, P. Masek, J. Hosek, S. Andreev, P. Dvorak, and R. Josth, "Emerging 5g applications over mmwave: Hands-on assessment of wigig radios," in *2017 40th International Conference on Telecommunications and Signal Processing (TSP)*, pp. 86–90, IEEE, 2017.

[6] X. Zhao, Q. Wang, S. Li, S. Geng, M. Wang, S. Sun, and Z. Wen, "Attenuation by human bodies at 26-and 39.5-GHz millimeter wavebands," *IEEE Antennas and Wireless Propagation Letters*, vol. 16, pp. 1229–1232, 2016.

[7] K. Sato, H. Kozima, H. Masuzawa, T. Manabe, T. Ihara, Y. Kasashima, and K. Yamaki, "Measurements of reflection characteristics and refractive indices of interior construction materials in millimeter-wave bands," in *1995 IEEE 45th Vehicular Technology Conference. Countdown to the Wireless Twenty-First Century*, vol. 1, pp. 449–453 vol.1, July 1995.

[8] K. Turbic, S. J. Ambroziak, and L. M. Correia, "A body-shadowing model for off-body and body-to-body communications," in *2018 Baltic URSI Symposium (URSI)*, pp. 53–54, May 2018.

[9] K. Zeman, J. Hosek, and L. M. Correia, "Designing Off-Body Propagation Channel Model for mmWave Indoor Communications," *IEEE Access; Under the review (Submitted 07/2019)*, vol. XX, no. X, pp. 1–8, 2017.

[10] K. Zeman, P. Masek, M. Stusek, J. Hosek, and P. Silhavy, "Accuracy comparison of propagation models for mmwave communication in ns-3," in *2017 9th International Congress on Ultra Modern Telecommunications and Control Systems and Workshops (ICUMT)*, pp. 334–340, Nov 2017.

[11] K. Zeman, M. Stusek, P. Masek, J. Hosek, and J. Sedova, "Enhanced 3d propagation loss model for mmwave communications," in *2018 10th International Congress on Ultra Modern Telecommunications and Control Systems and Workshops (ICUMT)*, pp. 1–7, IEEE, 2018.

[12] K. Zeman, M. Stusek, P. Masek, and J. Hosek, "Improved nlos propagation models for wireless communication in mmwave bands," in *2018 8th International Conference on Localization and GNSS (ICL-GNSS)*, pp. 1–6, IEEE, 2018.

[13] M. Mezzavilla, S. Dutta, M. Zhang, M. R. Akdeniz, and S. Rangan, "5G mmWave Module for the NS-3 Network Simulator," *Proceedings of the 18^{th} ACM International Conference on Modeling, Analysis and Simulation of Wireless and Mobile Systems - MSWiM '15*, 2015.

Curriculum Vitae

Ing. Krystof Zeman

Affiliation

Date of birth:	17.2.1991
Address:	Domamysl 39, Czech Republic
E-mail:	xzeman43@vutbr.cz xzeman43@stud.feec.vutbr.cz krystof.zeman@gmail.com
Tel:	+420 541 146 964 +420 602 468 470
WWW:	`https://www.vutbr.cz/lide/krystof-zeman-134671` `https://www.linkedin.com/in/krystof-zeman-21615a96/`

QUALIFICATION AND PROFESSIONAL CAREER

Current position

2015–up to now	Junior researcher with the Department of Telecommunications, Faculty of Electrical Engineering and Communication (FEEC), Brno University of Technology (BUT)

Qualification

2015–2019 (planned)	Ph.D. in Teleinformatics, BUT, Doctoral thesis: *Modeling of mmWave Propagation Channel for Off-body Communication Scenarios*
2013–2015	MSc. in Telecommunication and Information Technology, BUT, Diploma thesis: *Implementation of the Wireless M-Bus protocol into the NS-3 simulation environment*
2010–2013	Bc. in Teleinformatics, BUT, Bachelor thesis: *Designing Desktop Applications Using the Windows Workflow Foundation Library*

Professional career

2014–up to now	Member of the research group WISLAB (Wireless System Laboratory of Brno) Link: `http://www.wislab.cz`
2013–up to now	Junior researcher within the SIX Research Centre Link: `http://www.six.feec.vutbr.cz/`

PROFESSIONAL ACTIVITIES

Specialization	Research and development in the area of ultra-high speed wireless networks (Millimeter Wave), M2M / H2H communication, Industry 4.0,next-generation (5G) networks, Internet of Things and energy constrained devices Author / co-author of experimental prototypes developed within the contractual research for premier ICT companies (Konica Minolta, Vodafone, Telekom Austria Group, etc.).
Scientific internships	Tampere University, Tampere, Finland, Ph.D. exchange stay; (10/2014 – 11/2015) Instituto Superior Tecnico, Lisbon, Portugal, Ph.D. exchange stay; (4/2018 – 9/2018)

Membership in scientific and technical program committee international conferences	International Congress on Ultra-Modern Telecommunications and Control Systems ICUMT (workshop chair, 2015 - up to now).

Designated reviewer

- International Conference on Telecommunications and Signal Processing (WoS/Scopus, Conference)
- IEEE Wireless Communications Letters (IF: 2.449, Journal; ISSN: 2162-2337)

Teaching activities

2015 – 2018	Assistant lecturer, Computers and Programming 1 (laboratories, BUT)
2015 – 2018	Assistant lecturer, Computers and Programming 2 (laboratories, BUT)

OTHER QUALIFICATIONS AND KNOWLEDGE

Language knowledge	Czech language (native speaker) English language (level C1) German language (level A1)

Certifications

- HCSP: Hillstone Certified Security Professional (Aug 2017)
- CCNA Exploration: LAN Switching and Wireless, Brno University of Technology, FEEC (May 2012)
- CCNA Exploration: Accessing the WAN, Brno University of Technology, FEEC (May 2012)
- CCNP ROUTE: Implementing IP Routing, Brno University of Technology, FEEC

(December 2012)

Awards

• 1st Place at Inter-university Student Competition (MUNISS 2016).
Topic: *Realization of Smart City Vision for City District Novy Liskovec*

RESEARCH PROJECTS

Project participant (selected projects)

• 29840 iAuto5 – 2017

• 26610 Smart Multi-Purpose Home Gateway 2.0 – proof of concept demonstrator 2015

• 28457 Vyzkum informacnich a komunikacnich systemu a jejich bezpecnost

• 30854 Zarizeni pro vzdalene odecty fyzikalnich velicin

SELECTED PUBLICATIONS (2013 – 2017)

Selected publications in scientific journals with impact factor according to Web of Science

• MASEK, P.; HOSEK, J.; ZEMAN, K.; STUSEK, M.; KOVAC, D.; CIKA, P.; MASEK, J.; ANDREEV, S.; KROPFL, F. Implementation of True IoT Vision: Survey on Enabling Protocols and Hands-on Experience. International Journal of Distributed Sensor Networks, 2016, vol. 2016, no. 4, p. 1-18. ISSN: 1550-1329. (VaV ID 122369))

• MAŠEK, P.; MOKROV, E.; ZEMAN, K.; PONOMARENKO-TIMOFEEV, A.; PYATTAEV, A.; NESTEROV, S.; ANDREEV, S.; HOŠEK, J.; SAMOUYLOV, K.; KOUCHERYAVY, Y. A Practical Perspective on 5G-Ready Highly Dynamic Spectrum Management with LSA. Wireless Communications and Mobile Computing, 2018, vol. 2018, no. 1, p. 1-9. ISSN: 1530-8677. (VaV ID 148947)

SELECTED PRODUCTS (2013 – 2017)

• MASEK, P.; STUSEK, M.; ZEMAN, K.; MASEK, J.; KREJCI, J.; HOSEK, J.: G-WMBUS-02; Univerzalni testovaci zarizeni pro prenos Wireless M-BUS dat. T12, SE5.118.. URL: http://wislab.cz/our-work/universal-tester-for-wireless-m-bus-data-transmissions. (prototyp)

• ZEMAN, K.; STUSEK, M.; POKORNY, J.; MASEK, P.; HOSEK, J.: Home 4.0; Voice-assisted Smart Home within the Internet of Things Platform. Kancelar SE5.124, Technicka 12, 616 00 Brno. URL: http://www.wislab.cz

• MASEK, P.; STUSEK, M.; ZEMAN, K.; MASEK, J.; KREJCI, J.; HOSEK, J.: R-WMBUS-01; Generator M2M dat bezdratoveho komunikacniho protokolu Wireless M-BUS v sitich SmartGrid. T12, SE5.118. URL: http://wislab.cz/our-work/m2m-data-generator-utilizing-comunication-protocol-wireless-m-bus-within-the-smartgrid-infrastructure. (software)

• HOSEK, J.; MASEK, P.; KOVAC, D.; CIKA, P.; STUSEK, M.; ZEMAN, K.: OSGi Smart Hub 1.0; OSGi-based Smart Hub Platform. Ustav Telekomunikaci, Technicka 12, Brno. URL: http://wislab.cz/our-work/.

SUMMARY OF PUBLICATION ACTIVITIES

- Scientific journals with impact factor according to Web of Science: **2**
- International conferences indexed in Web of Science or Scopus: **30**
- Total number of citations according to Web of Science: **79**
- H-index according to Scopus: **5**
- H-index according to Web of Science: **3**
- Number of released products: **5**

REFERENCES

Prof. Luis M. Correia
Vice-President of IST; Coordinating Researcher of INOV-INESC
Department of Electrical and Computer Engineering (DEEC)
Av. Rovisco Pais 1, 1049-001 Lisboa, Portugal
Email: luis.m.correia@tecnico.ulisboa.pt

Prof. Yevgeni Koucheryavy
Head of W.I.N.T.E.R research lab & Senior IEEE Member
Department of Electronics and Communication Engineering
Tampere University, Korkeakoulunkatu 1, 33720
Email: yk@cs.tut.fi